

Technical Report No. 9

Modelling the marine CO₂ system in BALTSEM

January 2013

Erik Gustafsson



Baltic Nest
Institute

The Baltic Nest Institute

The Baltic Nest Institute host the Nest model, a decision support system aimed at facilitating adaptive management of environmental concern in the Baltic Sea.

Nest can be used to calculate required actions needed to attain politically agreed targets for the Baltic Sea ecosystem. By modeling the entire drainage area, Nest is a novel tool for implementing the ecosystem approach in a large marine ecosystem. The main focus of the model is on eutrophication and the flows of nutrients from land to sea.

Reducing the nutrient input to the sea and thus decreasing the negative environmental impacts is a politically prioritized area of international cooperation. Baltic Nest Institute can contribute to this process by formulating policies that are fair, transparent and cost-efficient. The main target group for the Nest Decision Support System is HELCOM and regional water directors in the riparian countries.

Technical Report No. 9
Modelling the marine CO₂ system in BALTSEM
Author: Erik Gustafsson
ISBN: 9978-91-86655-08-2
Layout: Marmar Nekoro

Baltic Nest Institute

Stockholm University Baltic Sea Centre, Stockholm University, Sweden
Address: Baltic Nest Institute, Stockholm University, SE-106 91 Stockholm, Sweden
www.balticnest.org

Previous reports in the BNI Technical Report Series

1. Revision of the country allocation of nutrient reductions in the Baltic Sea Action Plan (June 2009, ISBN 978-91-86655-00-6)
2. Validation data set compiled from Baltic Environmental Database (January 2011, ISBN 978-91-86655-01-3)
3. NANI/NAPI Calculator Toolbox Version 2.0 Documentation: Net Anthropogenic Nutrient Inputs in the Baltic Sea Catchment (January 2011 ISBN 978-91-86655-02-0)
4. Load scenarios for ECOSUPPORT (June 2011, ISBN 978-91-86655-03-7)
5. External nutrient loads to the Baltic Sea 1970-2006 (April 2012, ISBN 978-91-86655-04-4)
6. Long-term reconstruction of nutrient loads to the Baltic Sea, 1850-2006 (June 2012, ISBN 978-91-86655-05-1)
7. BALTSEM - a marine model for decision support within the Baltic Sea region (July 2012, ISBN: 978-91-86655-06-8)
8. Secchi depth calculations in BALTSEM (October 2012, ISBN: 978-91-86655-07-5)

Modelling the marine CO₂ system in BALTSEM

Erik Gustafsson

Baltic Nest Institute, Stockholm University, Stockholm, Sweden

BNI Technical report No. 9

Table of Contents

1. Introduction	3
2. Methods	4
2.1. Modelling the CO ₂ system	4
2.2. Biogeochemical processes	5
2.2.1. Primary production	5
2.2.2. Aerobic mineralization	6
2.2.3. Anaerobic mineralization	6
2.2.4. Production of hard parts	7
2.2.5. Burial	7
2.2.6. Organic alkalinity	7
2.3. Forcing	8
2.3.1. Air-sea CO ₂ exchange	8
2.3.2. River loads	10
2.3.3. Wet deposition of DIC	10
2.3.4. Lateral boundary conditions	11
2.4. Data	12
3. Results and discussion	15
3.1. Model calibration	15
3.2. Seasonal dynamics	16
3.3. Budget calculations	19
4. Conclusions	20
5. Acknowledgements	20
References	21
Appendix A	24
Calculating pH and pCO ₂	24
Appendix B	26
Calculating calcite and aragonite saturation states	26

1. Introduction

The main intention of this report is to give a general description of how the marine CO₂ system is incorporated into BALTSEM, a coupled physical-biogeochemical Baltic Sea model (cf. Savchuk et al., 2012). The CO₂ system involves four parameters; dissolved inorganic carbon (DIC or C_T), total alkalinity (TA or A_T), CO₂ partial pressure (pCO₂), and pH. If any two of these parameters are known (together with other state variables such as temperature and salinity), the other two can be calculated. DIC and alkalinity are chosen as model state variables as they are conservative with regard to changes in temperature and salinity (as opposed to pCO₂ and pH that are strongly dependent especially on temperature). A comprehensive description of the marine CO₂ system in general, and the Baltic Sea CO₂ system in particular, is given by Schneider (2011). Furthermore, all definitions and calculations employed are described in detail by Dickson et al. (2007).

Alkalinity and DIC are mainly transported to the Baltic Sea from rivers, but also from the North Sea. Alkalinity can be produced or consumed by different biogeochemical processes (Section 2.2.1-2.2.6), and is in addition transported to the North Sea through the open boundary in Northern Kattegat. DIC is assimilated by phytoplankton and again released when organic carbon is mineralized. Burial of freshly produced organic material is a permanent sink for carbon, but the major carbon sink is outflow to the North Sea (Kuliński and Pempkowiak, 2011). Differences in CO₂ partial pressure between atmosphere and surface water together with wind speed determine the CO₂ uptake or outgassing in different sub-basins (Section 2.3.1). The magnitude and direction of air-sea CO₂ exchange varies between sub-basins and also seasonally within basins (e.g. Kuliński and Pempkowiak, 2011; Schneider, 2011). The Gulf of Bothnia has earlier been described as a source of CO₂ to the atmosphere (Algesten et al., 2006), whereas conflicting results have been reported for the Baltic Proper (cf. Kuliński and Pempkowiak, 2011).

Formation and precipitation of calcium carbonate (CaCO₃) is a sink term for alkalinity and DIC, whereas dissolution of CaCO₃ on the other hand is a source term for both variables. In the Baltic Proper as well as the eastern and northern gulfs, formation of CaCO₃ seems to be negligible. The reason is believed to be unsaturation of calcite and aragonite mineral forms of CaCO₃ in winter and early spring (Tyrrell et al., 2008). In the Kattegat and Belt Sea, calcite seems to be oversaturated throughout the year, and the coccolithophore *Emiliania Huxleyi* can at times form massive blooms in the Skagerrak-Kattegat area (Blanz et al., 2005). Nevertheless, precipitation and dissolution of CaCO₃ are at this point not included as processes in the model, but may be a topic for future studies. A short description of how calcite and aragonite saturation states (Ω_{CA} and Ω_{AR}) are calculated is presented in Appendix B.

Below, the main processes that affect the concentrations of DIC and alkalinity are discussed in detail (Section 2.2). This is followed by a description of model forcing and boundary conditions (Section 2.3), and an overview of the available observations of CO₂ system parameters (Section 2.4). Model performance on both long-term average scale (Section 3.1), and on short-term scale (Section 3.2) is analysed in terms of comparisons between model results and observations. Finally, budget calculations reveal the overall main source and sink terms of both DIC and alkalinity in the Baltic Sea (Section 3.3).

2. Methods

2.1. Modelling the CO₂ system

To determine the inorganic carbon system, DIC and alkalinity are included as state variables in the BALTSEM model (for a detailed description of BALTSEM, see Savchuk et al., 2012). However, as DIC is highly influenced by production and mineralization of organic carbon, the major particulate and dissolved organic carbon species must be included as well. In this version of BALTSEM, four dissolved organic carbon (DOC) state variables – labile and refractory fraction of both autochthonous and allochthonous DOC – are together with autochthonous and allochthonous detrital and benthic carbon added as new state variables (Table 1). In addition, all plankton groups contain particulate organic carbon. Hydrogen sulphide is modelled as a separate state variable in order to account for alkalinity sources and sinks during anoxic conditions.

Table 1. Model state variables included to determine carbon fluxes in BALTSEM.

Notation	Meaning	Unit
Pelagic		
C_T	Dissolved inorganic carbon	$\mu\text{mol kg}^{-1}$
A_T	Alkalinity	$\mu\text{mol kg}^{-1}$
H_2S_T	Hydrogen sulphide	$\mu\text{mol kg}^{-1}$
$DETC_M$	Carbon detritus (autochthonous)	mg C m^{-3}
$DETC_T$	Carbon detritus (allochthonous)	mg C m^{-3}
$DOCL_M$	Labile autochthonous DOC	mg C m^{-3}
$DOCR_M$	Refractory autochthonous DOC	mg C m^{-3}
$DOCL_T$	Labile allochthonous DOC	mg C m^{-3}
$DOCR_T$	Refractory allochthonous DOC	mg C m^{-3}
Benthic		
$BENC_M$	Benthic organic carbon (autochthonous)	mg C m^{-2}
$BENC_T$	Benthic organic carbon (allochthonous)	mg C m^{-2}

Dissolved CO₂ and carbonic acid (H₂CO₃) are difficult to separate analytically, these two species are thus combined:

$$[CO_2^*] = [CO_2] + [H_2CO_3] \quad (2.1)$$

DIC is then defined as:

$$C_T = [CO_2^*] + [HCO_3^-] + [CO_3^{2-}] \quad (2.2)$$

The definition of alkalinity follow that by Dickson (1981):

$$A_T = [HCO_3^-] + 2[CO_3^{2-}] + [B(OH)_4^-] + [OH^-] + [HPO_4^{2-}] + 2[PO_4^{3-}] + [SiO(OH)_3^-] + [NH_3] \\ + [HS^-] - [H^+] - [HF] - [H_3PO_4] + [organic\ alkalinity] \quad (2.3)$$

In BALTSEM, alkalinity is determined by the expression above with the exception that organic alkalinity is not included (cf. Section 2.2.6) since the magnitude of this term is unclear (Ulfsbo et al., 2011).

Though pCO_2 and pH are not state variables, their values can be calculated at any moment using DIC, alkalinity, temperature, salinity, and concentrations of a few other state variables. The definition of pH is as follows

$$[H^+] = 10^{-pH} \leftrightarrow pH = -\log_{10}([H^+]) \quad (2.4)$$

The partial pressure of CO_2 is calculated from the $[CO_2^*]$ concentration and the temperature and salinity dependent solubility constant K_0 :

$$pCO_2 = \frac{[CO_2^*]}{K_0} \quad (2.5)$$

Details for the calculations of pH and pCO_2 are outlined in Appendix A.

2.2. Biogeochemical processes

Alkalinity is affected by several biogeochemical processes; nitrate and ammonium based primary production, mineralization, nitrification, denitrification, sulphate reduction, and sulphide oxidation. All these processes are modelled according to the descriptions by Wolf-Gladrow et al. (2007). The processes accounted for in BALTSEM are described below. In these examples, Redfield stoichiometry is used and the changes in alkalinity and DIC resulting from different processes are calculated (Table 2).

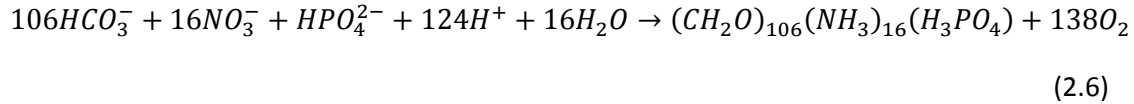
Table 2. Changes in DIC and alkalinity using the stoichiometry of Equation 2.6-2.12.

Process	Equation	ΔC_T	ΔA_T
Nitrate based production	2.6	-106	17
Ammonium based production	2.7	-106	-15
Aerobic mineralization	2.8	106	15
Nitrification	2.9	± 0	-32
Denitrification	2.10	106	99.8
Sulphate reduction	2.11	106	121
Sulphide oxidation	2.12	± 0	-106

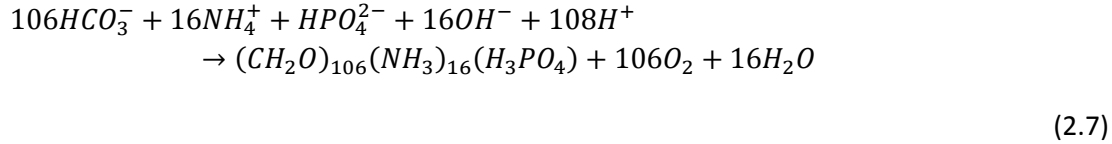
2.2.1. Primary production

The effect of phytoplankton production depends on the nitrogen source. When nitrate or nitrite is assimilated, alkalinity increases as $[H^+]$ is co-assimilated in order to maintain electroneutrality within the cell (Wolf-Gladrow et al., 2007). If ammonium on the other hand is the nitrogen source, alkalinity decreases because of a simultaneous uptake of $[OH^-]$. Nitrogen fixation, finally, does not (directly) affect alkalinity.

Production based on nitrate



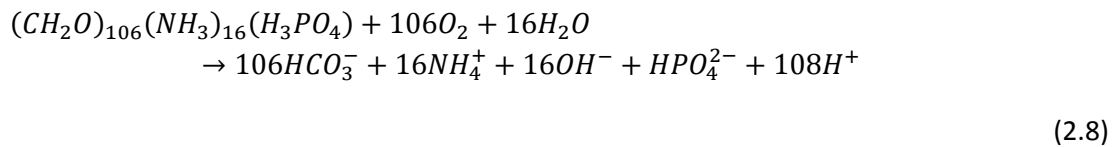
Production based on ammonium



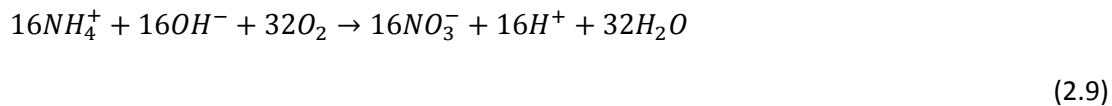
2.2.2. Aerobic mineralization

Mineralization of organic material increases alkalinity as hydroxide is released together with ammonium. If dissolved oxygen is present in the water, the ammonium will subsequently be oxidised into nitrate. Nitrification decreases alkalinity partly because of $[\text{OH}^-]$ removal and partly because of $[\text{H}^+]$ release. If organic material that was produced with nitrate as nitrogen source is completely mineralized and all released ammonium nitrified, the net effect on alkalinity is zero. There may however be a vertical displacement of alkalinity due to mixing and sedimentation – production, mineralization and nitrification in general do not occur at the same depths (cf. Edman and Omstedt, 2013). If organic material based on ammonium or atmospheric nitrogen is completely mineralized and nitrified, the net effect is that alkalinity decreases.

Mineralization



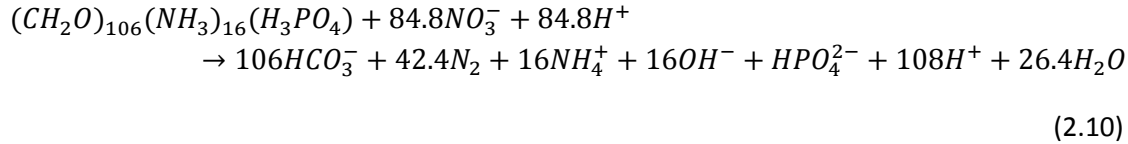
Nitrification



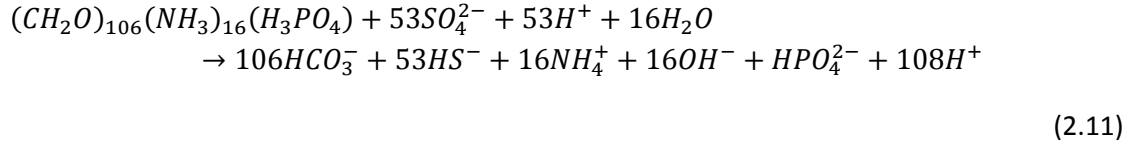
2.2.3. Anaerobic mineralization

If all dissolved oxygen is consumed, nitrate can be used to oxidise organic material. As nitrate is removed, a simultaneous loss of $[\text{H}^+]$ results in a net alkalinity source associated with denitrification. Metal oxides such as manganese dioxide (MnO_2) and iron oxy-hydroxide (FeOOH) may also be reduced in the absence of dissolved oxygen resulting in increased alkalinity (e.g. Ulfsbo et al., 2011). Concentrations of these species are however normally negligible and reduction of metal oxides is for that reason not included in BALTSEM. Instead, when both oxygen and nitrate are depleted, sulphate is used to oxidise organic material. Sulphate reduction is a large alkalinity source, but as the anoxic water is again supplied with oxygen, most sulphide is oxidised and the net effect on alkalinity of anoxic-oxic transitions is thus dampened. In the Belt Sea, Kattegat and Skagerrak region, Jørgensen et al. (1990) estimated that between 4-32% of the sulphide produced during anoxic conditions was permanently buried as pyrite. In this study, it is assumed that 70% of the sulphide produced during anoxic conditions is re-oxidized and the remaining 30% buried. Thus, anoxic conditions results in a net alkalinity increase.

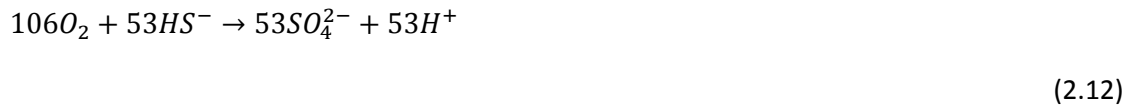
Denitrification



Sulphate reduction



Sulphide oxidation



2.2.4. Production of hard parts

The effect on alkalinity associated with biogenic silica production is assumed to be zero (Wolf-Gladrow et al., 2007). Production and dissolution of calcium carbonate shells, on the other hand, may have a large effect on alkalinity in some sea areas. As discussed above, calcifiers are not accounted for in the model (and apparently more or less absent except in the Kattegat and possibly the Belt Sea, cf. Tyrrell et al., 2008), and the effects of CaCO₃ precipitation/dissolution are thus not included.

Formation of biogenic silica



Formation of calcite/aragonite



2.2.5. Burial

Burial of organic nitrogen is a net alkalinity source, as the combined effect of mineralization and subsequent nitrification (that are prevented to occur if organic material is permanently lost from the system) is an alkalinity decrease.

2.2.6. Organic alkalinity

The possibly significant, but highly uncertain, influence on alkalinity related to dissolved organic carbon (DOC) production and mineralization is not included. It has been observed in other areas that DOC released by primary producers may increase the alkalinity, approximately by one alkalinity unit per DOC unit (Kim and Lee, 2009). Thus, during net primary production, the surface water may become slightly more buffered, resulting in a small pH increase and pCO₂ drop. When this DOC is subsequently mineralized, pCO₂ will be amplified and pH diminished; the overall effect of this organic alkalinity is thus an amplified seasonal cycle of both pCO₂ and pH. To the present author's knowledge, studies on the influence of DOC production/mineralization on Baltic Sea alkalinity have not been published.

2.3. Forcing

2.3.1. Air-sea CO₂ exchange

Gas exchange between ocean and atmosphere is controlled by the air-sea difference in CO₂ partial pressure and by the wind speed dependent transfer velocity. The exchange (mol kg⁻¹ cm h⁻¹) can be written (e.g. Wanninkhof et al., 2009):

$$F_{CO_2} = k_{wCO_2} K_0 (pCO_2^w - pCO_2^a) \quad (2.15)$$

Here, K_0 (mol kg⁻¹ atm⁻¹) is the CO₂ gas solubility (Weiss, 1974), whereas pCO_{2w} and pCO_{2a} (atm) are carbon dioxide partial pressure in surface water and air respectively. Several different parameterizations for the transfer velocity, k_{wCO_2} (cm h⁻¹), have been described in the literature. The transfer velocity not only depends on wind speed, but can also be influenced by mixed layer depth and atmosphere stratification (Rutgersson and Smedman, 2010). Nevertheless, the parameterization used in this study follows that by Weiss et al. (2007):

$$k_{wCO_2} = k_{660} \sqrt{\frac{660}{Sc}} \quad (2.16)$$

Here, k_{660} is the normalized transfer velocity (Wanninkhof et al., 2009), and Sc is a temperature dependent Schmidt number (Wanninkhof, 1992).

Atmospheric pCO₂

The Baltic Sea atmospheric CO₂ (pCO_{2a}) was constructed from observations at two other stations; Mauna Loa in Hawaii (1958-2008; <http://cdiac.ornl.gov/ftp/trends/co2/maunaloa.co2>), and Barrow in Alaska (1974-2007; <http://cdiac.ornl.gov/ftp/trends/co2/barrsio.co2>). Barrow is the northern hemisphere background station. On average, Baltic Sea atmospheric CO₂ exceeds Barrow station CO₂ by only 3 ppm (Schneider, 2011). Time series for Baltic Sea atmospheric CO₂ was constructed as follows: First, the linear trend over the 1974-2006 period was calculated for Barrow station (Figure 1, upper panel). Second, the average monthly anomaly (Figure 1, lower panel) was added to the linear trend. The concentrations in this constructed time series were increased by 3 ppm to achieve an approximation of Baltic Sea pCO_{2a} over the 1974-2006 period. In order to extend the time series backwards in time, the linear trend from Mauna Loa station was used (corrected for the average difference between Barrow and Mauna Loa, and also for the average difference between Baltic Sea and Barrow) over the 1958-1974 period together with the average monthly anomaly from Barrow. These two constructed time series were then combined to achieve Baltic Sea atmospheric CO₂ over the 1958-2006 period (Figure 2).

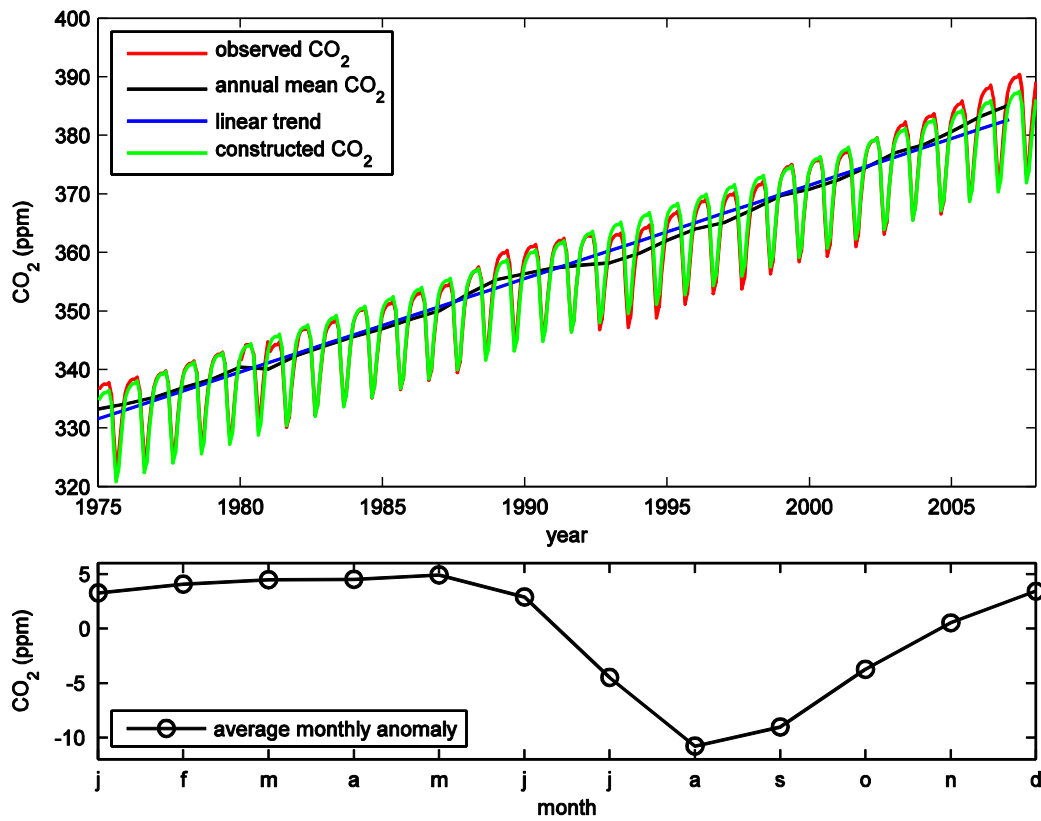


Figure 1. Atmospheric CO₂ (ppm) at the northern hemisphere background station Barrow in Alaska. Upper panel: observed CO₂ (red line), annual mean CO₂ (black line), linear trend (blue line), and constructed CO₂ = linearized mean value + average monthly anomaly (green line). Lower panel: average monthly anomaly.

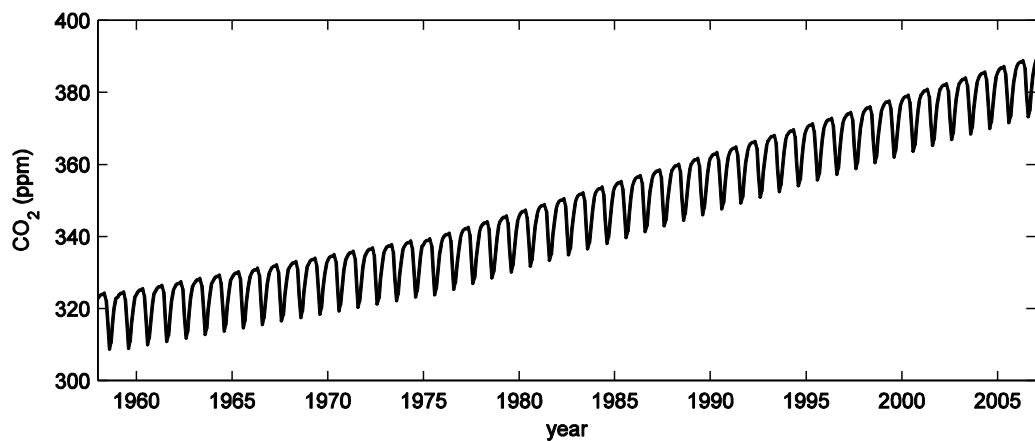


Figure 2. Constructed atmospheric CO₂ (ppm) for the Baltic Sea region over the 1958-2006 period.

2.3.2. River loads

Different geological structures in catchment areas around the Baltic Sea result in a wide range of riverine alkalinity and background DIC concentrations (Beldowski et al., 2010). Riverine DIC is in addition influenced by respiration and CO₂ exchange with the atmosphere (Humborg et al., 2009). Due to a limited amount of direct observations, it is at this point assumed that DIC and alkalinity (and also DOC) concentrations in river water have constant background values, and added to that average monthly anomalies. The average monthly anomalies were based on calculations from the watershed model CSIM (cf. Mörth et al., 2007), as applied in a coupled catchment-sea climate sensitivity study in the Baltic Sea (Omstedt et al., 2012). The estimated background concentrations (Table 3) are based on measurements, but tuned to fit model results to observations. Alkalinity data for Swedish rivers were achieved from SLU, the Swedish University of Agricultural Sciences (<http://www.slu.se/vattenmiljo>). For several sub-basins, the estimates were improved by adding additional alkalinity information from the literature. DIC concentrations were partly based on the estimated average riverine total inorganic carbon (TIC) concentrations by Kuliński and Pempkowiak (2011).

Table 3. Estimated average alkalinity and DIC concentrations (μmol kg⁻¹) in river water supplied to the different sub-basins.

Sub-basin	Alkalinity	DIC	Alkalinity reference
NK	230	310	SLU
CK	1000	1400	SLU, Gazeau et al. (2005)
SK	250	380	SLU
SB	2200	2500	Rebsdorf et al. (1991)
FB	2200	2500	Rebsdorf et al. (1991)
OS	2200	2500	
AR	2200	2500	SLU, Rebsdorf et al (1991)
BN	2200	2500	
GS	3400	3900	
BS	240	350	SLU, Saarinen et al. (2010)
BB	210	360	SLU, Saarinen et al. (2010)
GR	3600	4000	
GF	1300	1600	

2.3.3. Wet deposition of DIC

Atmospheric CO₂ dissolves in rainwater, resulting in a DIC source to the sea associated with precipitation. The DIC concentration in rainwater is given by

$$[CO_2^*]_{PR} = K_0 pCO_{2a} \quad (2.17)$$

where K_0 is the solubility constant (Weiss, 1974), and pCO_{2a} is CO₂ partial pressure in the atmosphere. Kuliński and Pempkowiak (2011) estimated that the average temperature in rainwater is approximately 10 °C. At this temperature, $K_0 \approx 0.05 \text{ mol l}^{-1} \text{ atm}^{-1}$. Between 1970 and 2006, the atmospheric CO₂ partial pressure increased from about 325 to 380 μatm, and the average DIC concentration in rainwater (assuming a temperature of 10 °C) has increased from 16 to 19 μmol l⁻¹ under the same period. The resulting annual DIC input has been of the order 4-5 Gmol C yr⁻¹, and this minor source can be neglected.

2.3.4. Lateral boundary conditions

During oxic conditions, salinity and alkalinity often show a linear correspondence, though the salinity/alkalinity relation may differ largely between different systems depending on e.g. river alkalinity (cf. Schneider et al., 2012). DIC concentrations generally follow alkalinity concentrations but are also affected by primary production and respiration. In order to generate boundary conditions for both alkalinity and DIC, these two state variables were assumed to correspond linearly to already existing salinity profiles:

$$A_T = 27S + 1330 \quad (2.18)$$

$$C_T = 27S + 1160 \quad (2.19)$$

The correspondence between observed alkalinity/DIC ($\mu\text{mol l}^{-1}$) and salinity at the station Anholt East is indicated by a comparison of annual mean concentrations (Figure 3). It can be seen that the assumption of linear correspondence between salinity and DIC is not optimal. DIC concentrations diverges from the linear relation in the deep water (high salinities) due to a net release of DIC associated with mineralization of organic carbon. In the surface water on the other hand DIC concentrations are drawn down due to a net DIC assimilation associated with primary production. Although alkalinity is also affected by biogeochemical processes, the influence is comparatively small during oxic conditions (cf. Table 2).

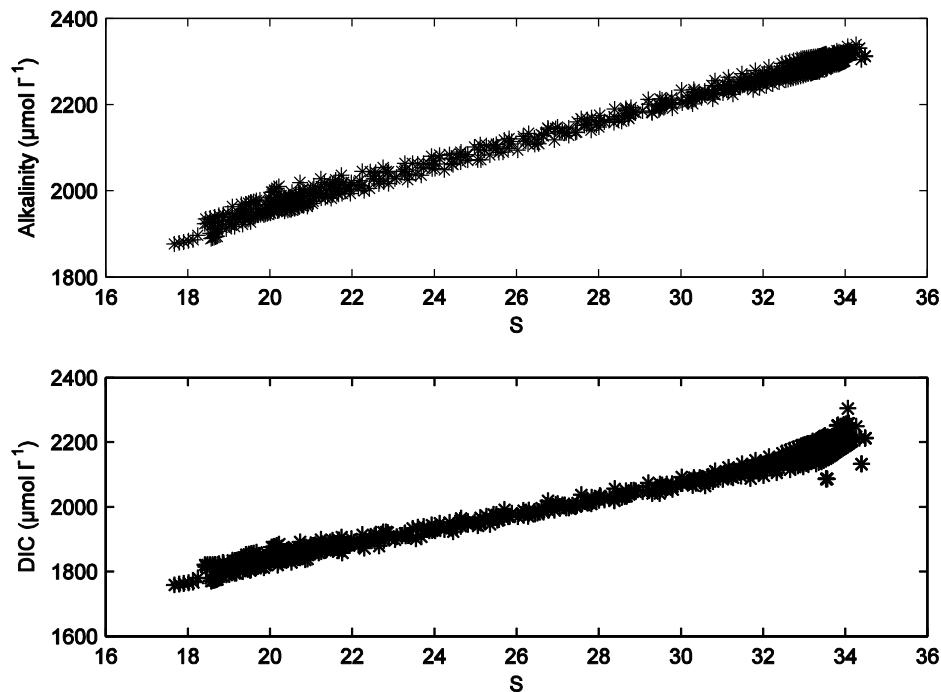


Figure 3. Annual mean observed alkalinity (upper panel) and DIC (lower panel) versus salinity at the station Anholt East in Southern Kattegat.

2.4. Data

Data were retrieved from the SHARK database, provided by the SMHI. In the model, it is the two state variables DIC and alkalinity that are used to calculate pH and pCO₂. However, it is usually only pH and alkalinity that are measured, which implies that “observed” DIC and pCO₂ have to be calculated from observed alkalinity and pH (and in addition e.g. temperature, salinity, and hydrogen sulphide).

One complication is that observations of pH from the SHARK database are reliable starting from 1993 (Andersson et al., 2008), and observations of alkalinity probably from 1995. Comparisons between model results and observations are thus restricted to the years between 1995 and 2006. Another complication is that alkalinity data extracted from the SHARK database suffer from a systematic error. Hydrogen sulphide was apparently already oxidized when the analyses were performed, resulting in an underestimated alkalinity in anoxic water samples (cf. Ulfso et al., 2011). Thus, measured alkalinity should be corrected according to:

$$A_{Tcorr} = A_{Tobs} + 2H_2S_T \quad (2.20)$$

In the expression above, A_{Tcorr} is corrected alkalinity, A_{Tobs} measured alkalinity, and H_2S_T measured hydrogen sulphide concentration ($\mu\text{mol l}^{-1}$). In the periodically anoxic parts of the deep water, the alkalinity generation from sulphate reduction is a major alkalinity source, as shown for the station BY15 in the Gotland Deep (Figure 4).

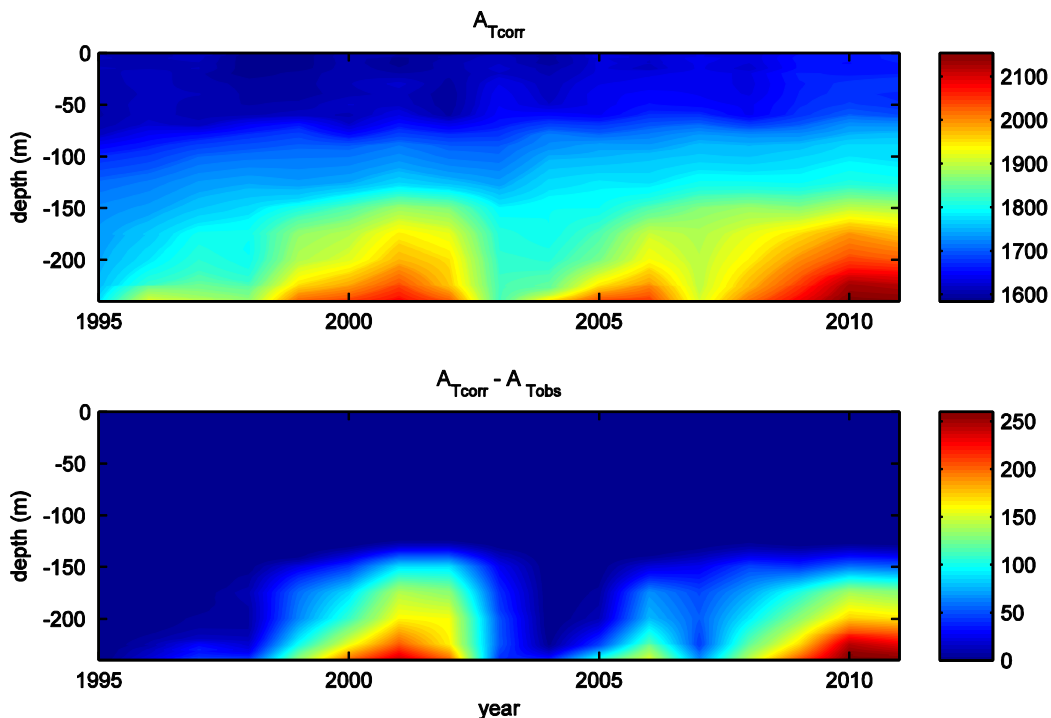


Figure 4. Annual mean alkalinity ($\mu\text{mol l}^{-1}$) at the station BY15. Upper panel: corrected alkalinity (cf. Equation 2.20). Lower panel: difference between corrected and measured alkalinity.

At a few stations – e.g. Anholt East in Southern Kattegat, BY5 in the Bornholm basin, and BY15 in the Gotland Sea – alkalinity and pH data is available with approximately monthly resolution from 1995 and onwards (Figure 5-7). Generally, highly resolved time series over longer time periods are however lacking for these parameters. This is especially the case in the Bothnian Sea and Bay (where data coverage for most variables is poor). The Gulfs of Riga and Finland, as well as Samsö and Fehmarn Belt are not covered by the SHARK database. However, the ICES database contains pH data for the Gulfs of Riga and Finland, whereas alkalinity data is very sparse in the Gulf of Finland and absent in the Gulf of Riga. pH data from the SHARK database are measured at the pH^{NBS} scale, whereas the calculations in BALTSEM are done using the pH^{tot} scale. The pH^{NBS} values are converted to pH^{tot} by subtracting 0.13 pH units (cf. Edman and Omstedt, 2013).

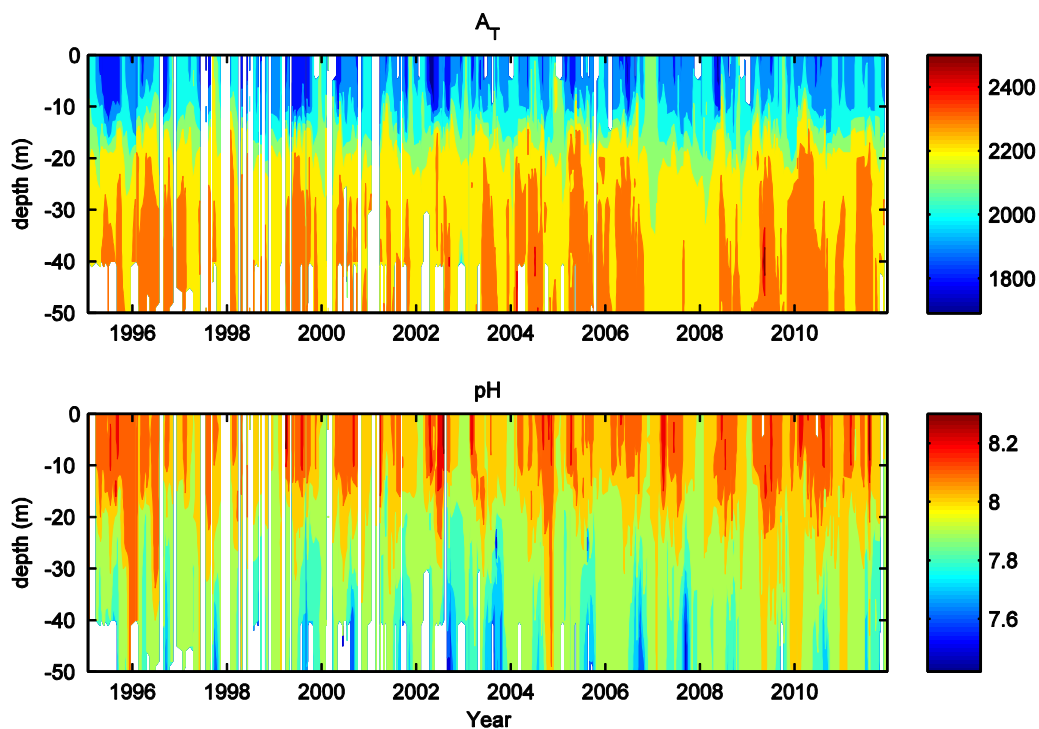


Figure 5. Observed alkalinity ($\mu\text{mol l}^{-1}$) and pH at Anholt East.

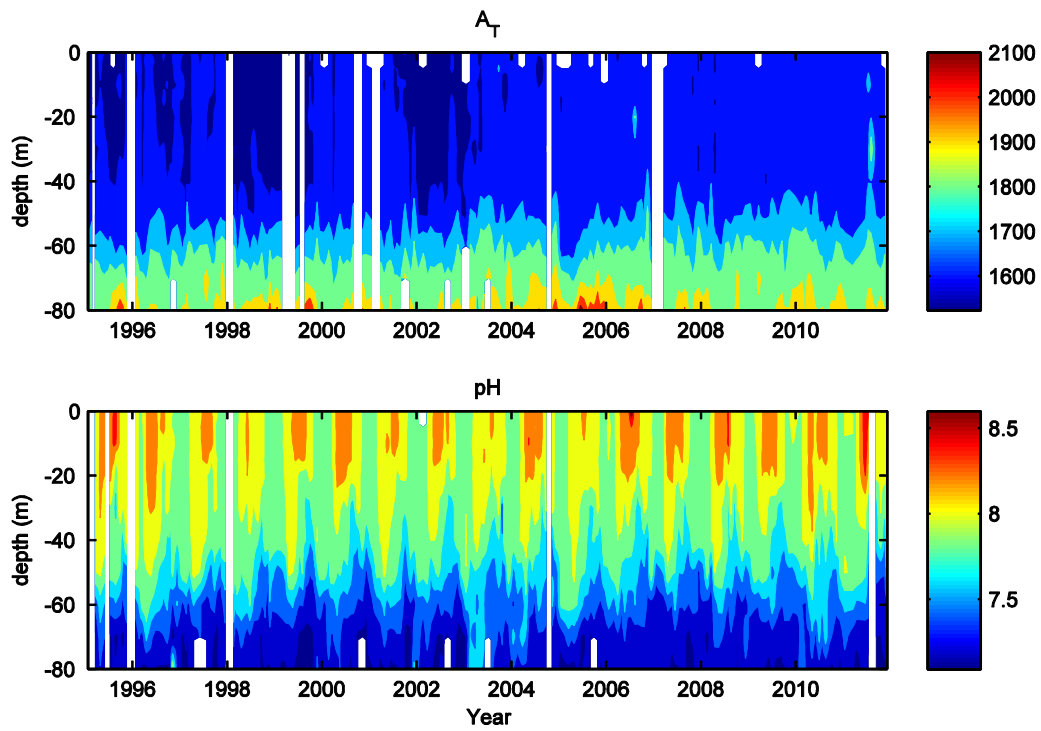


Figure 6. Observed alkalinity ($\mu\text{mol l}^{-1}$) and pH at BY5 in the Bornholm Basin.

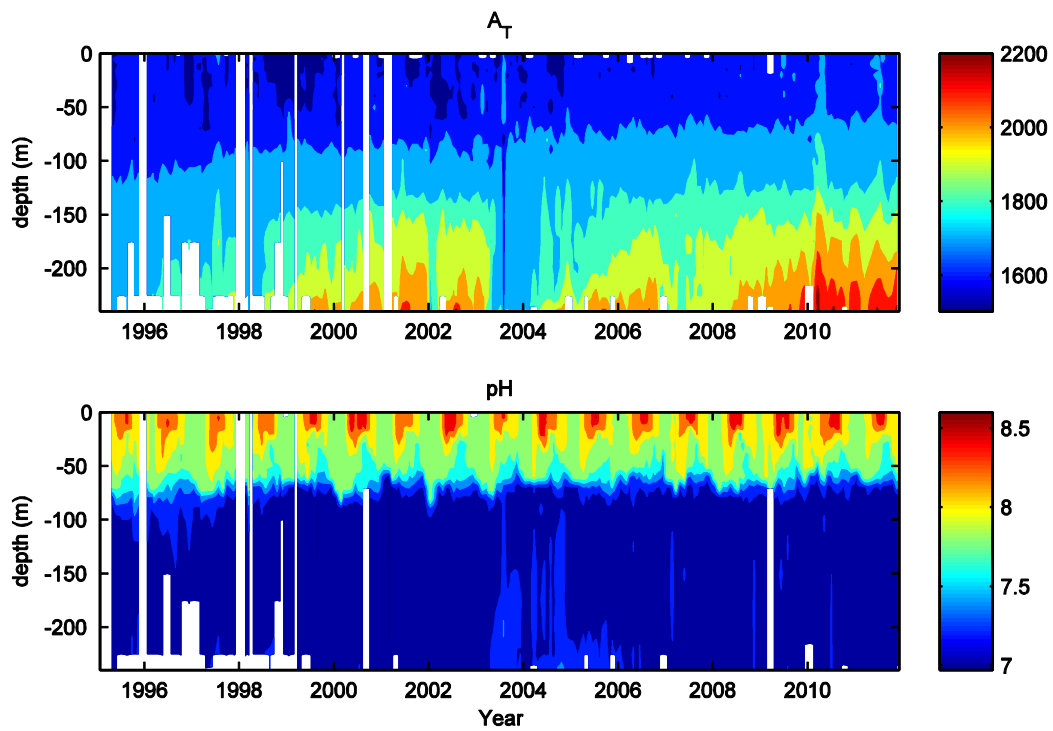


Figure 7. Observed alkalinity ($\mu\text{mol l}^{-1}$) and pH at BY15 in the Gotland Sea.

3. Results and discussion

3.1. Model calibration

To calibrate the model, average observed profiles for the four CO₂ system parameters over the 1995-2006 period were compared to average modelled profiles. Below, results are displayed for those sub-basins of the Baltic Sea where data coverage was comparatively good, i.e., the Southern Kattegat, Bornholm Basin and Gotland Sea (Figure 8-10).

Discrepancies between modelled and observed alkalinity can partly result from differences between modelled and observed salinities. Alkalinity is also highly influenced by transitions between oxic and anoxic conditions (Section 2.2.3). Thus, even small differences between modelled and observed oxygen can have large consequences for alkalinity when the oxygen concentration is close to zero. Furthermore, the assumption that alkalinity concentrations in rivers have constant background values is not optimal. Organic alkalinity may in addition have a so far unknown influence in the system.

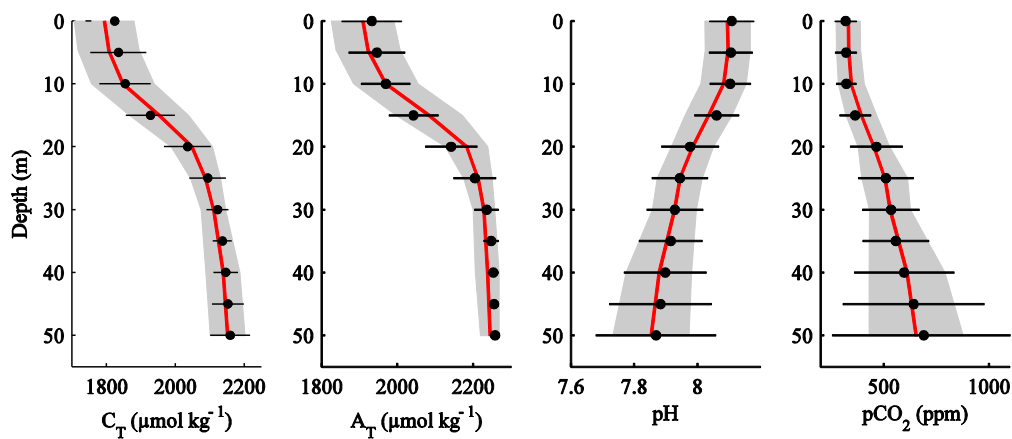


Figure 8. Comparison between observations at station Anholt E. and model results for the Southern Kattegat sub-basin covering the 1995-2006 period. Black dots indicate the average modelled value of a state variable at a certain depth and the black bars the corresponding standard deviation. Similarly, the red lines and shaded grey areas indicate the depth-dependent average value and standard deviation for observations. Results for DIC, alkalinity ($\mu\text{mol kg}^{-1}$), pH and $p\text{CO}_2$ (ppm) are displayed.

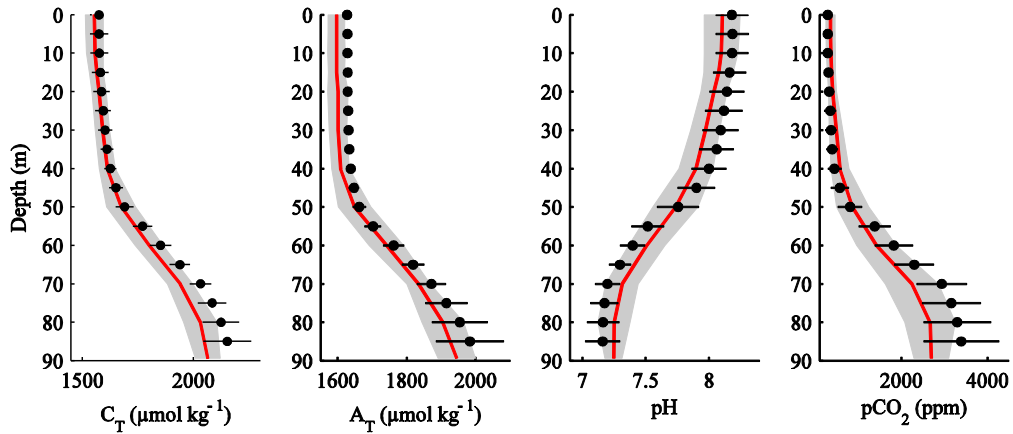


Figure 9. Same as Figure 8, but in this case observations at station BY5 are compared to model results from the Bornholm basin.

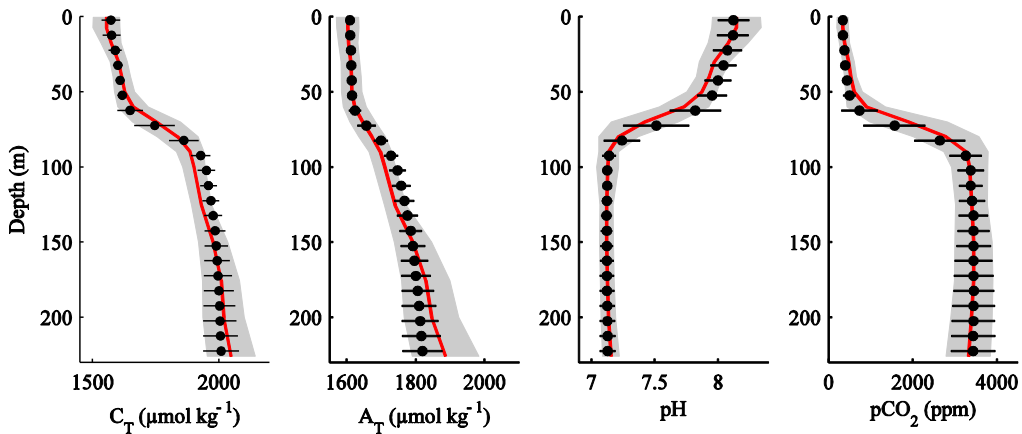


Figure 10. Same as Figure 8, but in this case observations at station BY15 are compared to model results from the Gotland Sea.

3.2. Seasonal dynamics

Long-term average results for the parameters of the CO₂ system correspond well to observations, at least in the sub-basins where data coverage is acceptable (cf. Section 3.1). In this section, seasonal and inter-annual dynamics of these parameters will be briefly discussed. Model results from the Gotland Sea are compared to observations from the station BY15 both for surface water (0 m, Figure 11) and deep water (200 m, Figure 12).

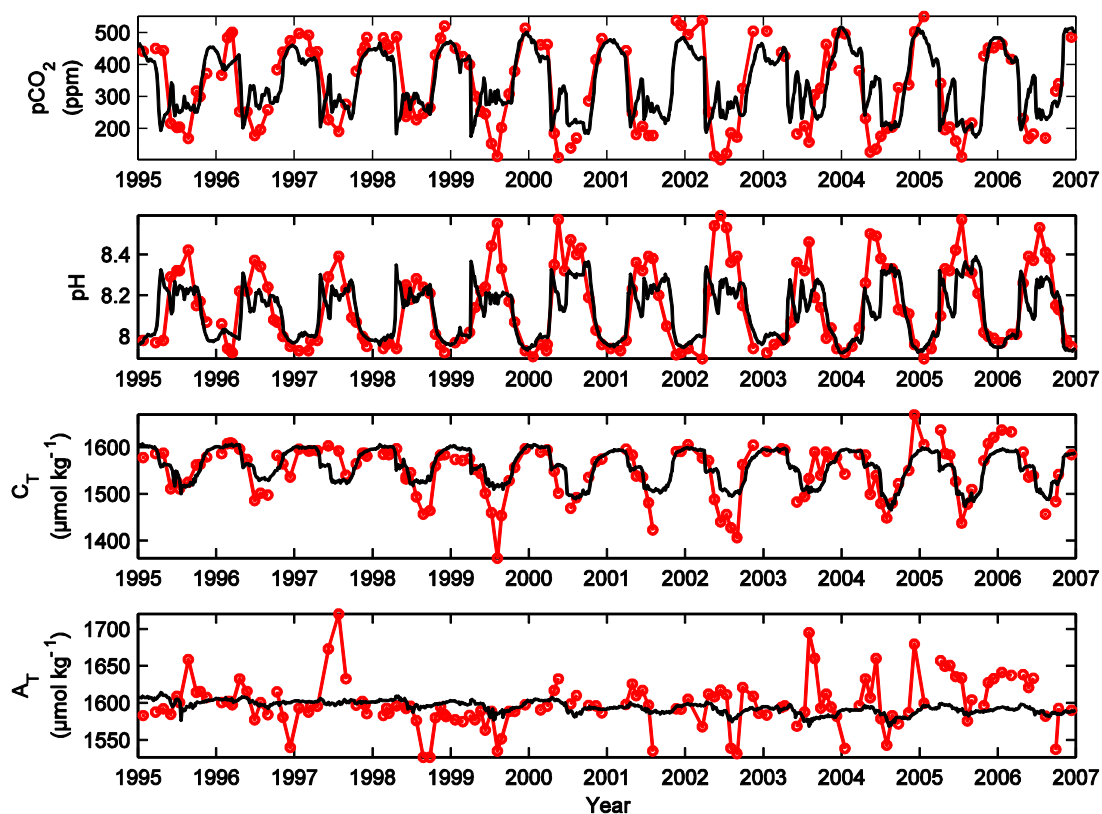


Figure 11. Comparison between observations at station BY15 (red circles) and model results from the Gotland Sea (black lines). The four panels display $p\text{CO}_2$ (ppm), pH, DIC, and alkalinity ($\mu\text{mol kg}^{-1}$) at the surface (0 m) during the 1995-2006 period.

Model results indicate a $p\text{CO}_2$ increase (and pH dip) between the spring bloom culmination and cyanobacteria onset (Figure 11). The reason is the increasing water temperature that influences solubility and dissociation constants. In the real Baltic Sea this temperature related increase in $p\text{CO}_2$ is somewhat compensated by a continuous DIC assimilation. In the model however, net phytoplankton production basically stops when nitrate is depleted during the spring bloom, and continues only when the water temperature is sufficiently high for cyanobacteria production.

This discrepancy between modelled and real Baltic Sea pH and $p\text{CO}_2$ could be explained by a so far unknown nitrogen source; e.g. “cold fixation” of atmospheric nitrogen (Schneider et al., 2009), or an effective utilization of dissolved organic nutrients (Korth et al., 2011). In addition, phytoplankton are to some extent able to migrate vertically to retrieve nutrients from below the photic zone. As noted above (Section 2.2.6), the seasonal cycles of $p\text{CO}_2$ and pH may also be influenced by organic alkalinity. The CO_2 system is in addition affected by excessive phytoplankton DIC uptake followed by DOC exudation (cf. Baines and Pace, 1991), and also adaptable cell stoichiometry as compared to constant Redfield ratios (e.g. Van Mooy et al., 2009).

Furthermore, there are compared to the rather stable modelled alkalinity large variations in observed alkalinity (Figure 11). These variations probably occur mainly as a result of horizontal advection of water masses of different origins (and different salinity). In the model, however, the

Gotland basin is assumed horizontally homogeneous, and fluctuations are consequently much smaller.

Due to the large alkalinity generation associated with both denitrification and sulphate reduction, deep water pH and $p\text{CO}_2$ are comparatively stable during anoxic stagnation periods (Figure 12). DIC concentrations are on the other hand steadily increasing during stagnation periods as a result of continuous degradation of organic carbon.

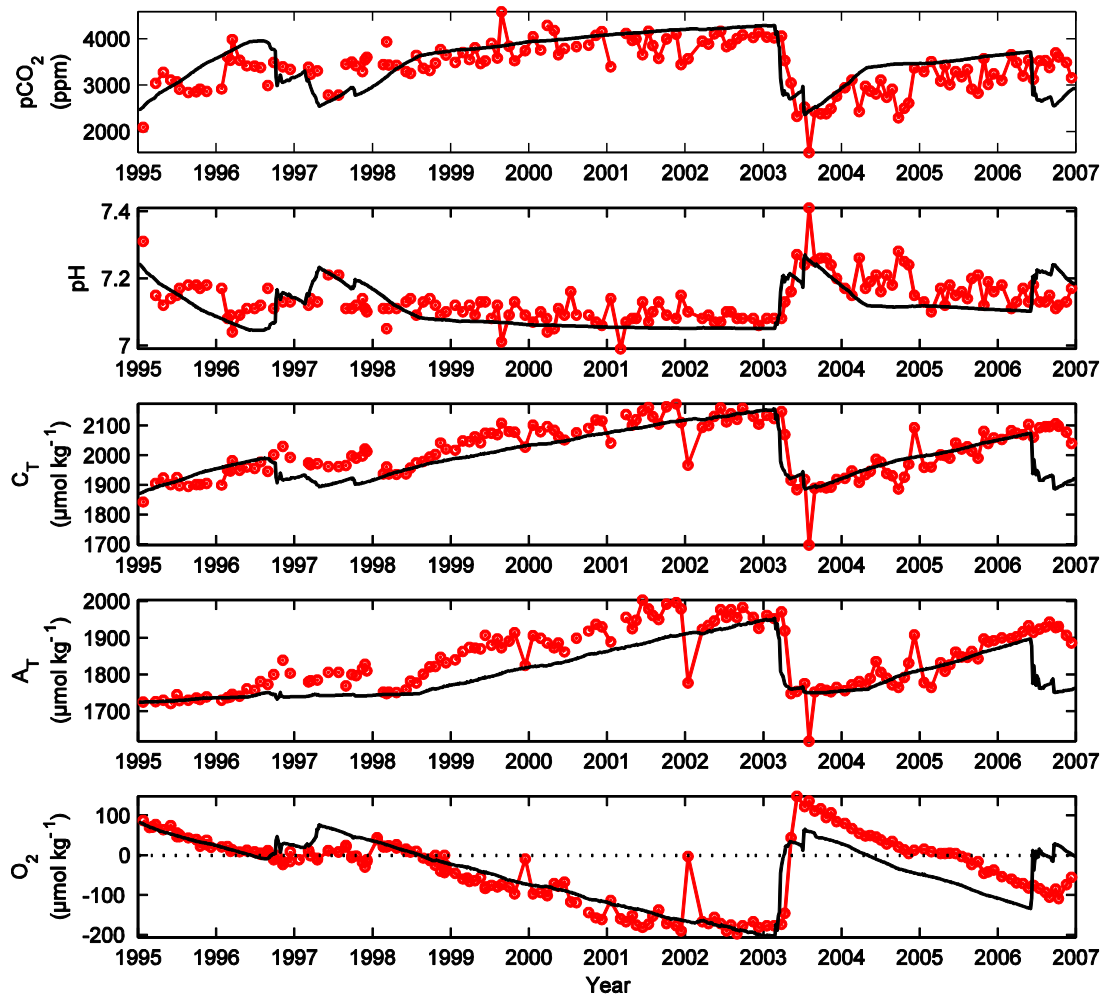


Figure 12. Comparison between observations (corrected alkalinity) at station BY15 (red circles) and model results from the Gotland Sea (black lines). The four panels display $p\text{CO}_2$ (ppm), pH, DIC, alkalinity, and oxygen ($\mu\text{mol kg}^{-1}$) in the deep water (200 m) during the 1995-2006 period.

3.3. Budget calculations

In this section, average source and sink terms for DIC and alkalinity covering the entire Baltic Sea over the 1980-2006 period are presented (Table 4).

Table 4. Average source and sink terms for DIC and alkalinity (Gmol yr^{-1}) over the 1980-2006 period.

	River load	Net air-sea exchange	Net advection	Internal SMS	Total SMS
DIC	820	150	-860	-130	-19
Alkalinity	680	-	-840	140	-22

River runoff is the main source term for both DIC and alkalinity, and the main loss term for both properties is net advection through the Kattegat-Skagerrak boundary. The internal source and sink terms for DIC are basically mineralization and production. Burial and advection of autochthonous organic carbon are indirect sink terms for DIC, whereas mineralization of allochthonous organic carbon is a net source term. The internal sources minus sinks (SMS) for DIC are on average negative, which indicates that burial and advection of autochthonous organic carbon exceeds mineralization of allochthonous organic carbon. Not only on seasonal, but also on annual scale, the Baltic Sea alters between being a source and a sink for atmospheric CO_2 according to the model results (Figure 13). Most years, however, uptake of CO_2 during the productive season exceeds outgassing during winter.

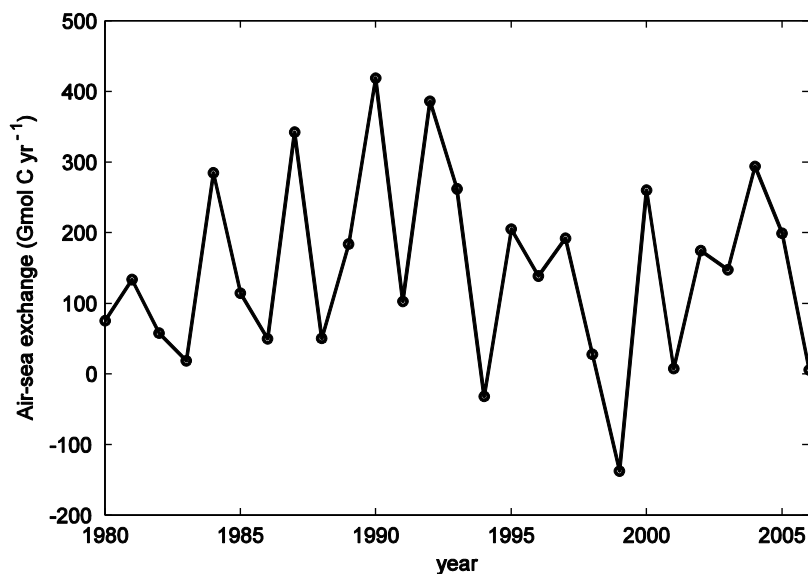


Figure 13. Annual air-sea CO_2 exchange (Gmol C yr^{-1}). Positive values indicate net uptake.

There are several different processes that contribute to the internal source and sink terms for alkalinity (cf. Section 2.2). On average, these internal processes together function as a source term for alkalinity, which mainly is a consequence of the effective denitrification in the Baltic Sea. Total sources minus sinks for both DIC and alkalinity are on average negative during the model period. Decreasing trends for the total amounts of alkalinity and DIC in the entire Baltic Sea are thus evident as well (Figure 14). This development is explained by decreasing trends in total river loads of DIC and alkalinity during the model period (not shown).

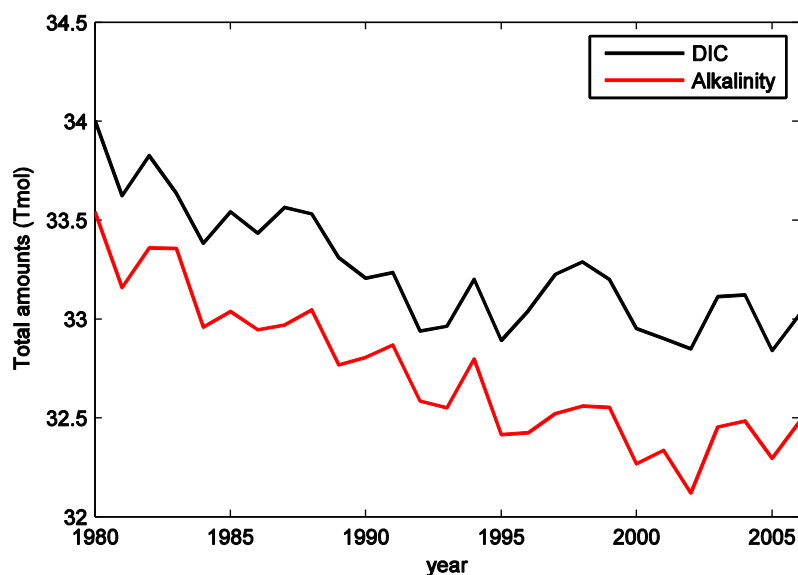


Figure 14. Total amounts of DIC and alkalinity (Tmol) in the Baltic Sea over the 1980-2006 period.

4. Conclusions

Large-scale and long-term modelled properties of the Baltic Sea CO₂ system are in good agreement with observations, although data series of reasonable resolution and continuity are only available for a few sub-basins (cf. Section 3.1). CO₂ partial pressure and pH vary largely on a seasonal basis (as exemplified by model results from the Gotland Sea and measurements from BY15, Section 3.2), both as a result of biogeochemical processes and variations mainly in temperature. The model is not yet capable of fully capturing the seasonal cycles of pCO₂ and pH, and the discrepancies are likely to occur partly due to shortcomings in parameterizations of some biological processes, and also due to the fact that some processes are so far largely unknown.

Budget calculations covering the entire Baltic Sea (Section 3.3) indicate that river runoff is the main source for both DIC and alkalinity, whereas advection out of the system is the main sink term for both properties. On average, the Baltic Sea acts as a sink for atmospheric CO₂, although there can be large differences from year to year (and also between different sub-basins). Large areas of the Baltic Sea deep water suffer from oxygen poor conditions, and one result of oxygen scarcity is an effective denitrification in the system (cf. Savchuk, 2010). Denitrification is a net source for alkalinity and dominates the internal source and sink terms in the Baltic Sea.

5. Acknowledgements

The Baltic Nest Institute is funded by the Swedish Ministry of Environment through the Swedish Agency for Marine and Water Management. Moa Edman developed the program used to calibrate model results for the various sub-basins (Section 3.1).

References

- Algesten, G., Brydsten, L., Jonsson, P., Kortelainen, P., Löfgren, S., Rahm, L., Råike, A., Sobek, S., Tranvik, L., Wikner, J., Jansson, M., 2006. Organic carbon budget for the Gulf of Bothnia. *Journal of Marine Systems* 63, 155–161.
- Andersson, P., Håkansson, B., Håkansson, J., Sahlsten, E., Havenhand, J., Thorndyke, M., Dupont, S., 2008. Marine Acidification - On effects and monitoring of marine acidification in the seas surrounding Sweden (Oceanografi No. 92). SMHI.
- Baines, S.B., Paice, M.L., 1991. The Production of Dissolved Organic Matter by Phytoplankton and its Importance to Bacteria: Patterns Across Marine and Freshwater Systems. *Limnology and Oceanography* 36, 1078–1090.
- Beldowski, J., Löffler, A., Schneider, B., Joensuu, L., 2010. Distribution and biogeochemical control of total CO₂ and total alkalinity in the Baltic Sea. *Journal of Marine Systems* 81, 252–259.
- Blanz, T., Emeis, K.-C., Siegel, H., 2005. Controls on alkenone unsaturation ratios along the salinity gradient between the open ocean and the Baltic Sea. *Geochimica et Cosmochimica Acta* 69, 3589–3600.
- Dickson, A.G., 1981. An exact definition of total alkalinity and a procedure for the estimation of alkalinity and total inorganic carbon from titration data. *Deep Sea Research Part A. Oceanographic Research Papers* 28, 609–623.
- Dickson, A.G., 1990. Thermodynamics of the dissociation of boric acid in synthetic sea water from 273.15 to 298.15 K. *Deep-Sea Research* 37, 755–766.
- Dickson, A.G., Riley, J.P., 1979. The estimation of acid dissociation constants in seawater media from potentiometric titrations with strong base. I. The ionic product of water—K_w. *Marine Chemistry* 7, 89–99.
- Dickson, A.G., Sabine, C.L., and Christian, J.R., 2007. Guide to best practices for ocean CO₂ measurements, Sidney, British Columbia, North Pacific Marine Science Organization, PICES Special Publication 3, 2007.
- Edman, M., Omstedt, A., 2013. Modeling the dissolved CO₂ system in the redox environment of the Baltic Sea. *Limnology and Oceanography* 58.
- Gazeau, F., Borges, A.V., Barrón, C., Duarte, C.M., Iversen, N., Middelburg, J.J., Delille, B., Pizay, M.D., Frankignoulle, M., Gattuso, J.P., 2005. Net ecosystem metabolism in a micro-tidal estuary (Randers Fjord, Denmark): evaluation of methods. *Marine Ecology Progress Series* 301.
- He, X., Wang, W.-X., 2006. Relative importance of inefficient feeding and consumer excretion to organic carbon flux from *Daphnia*. *Freshwater Biology* 51, 1911–1923.
- Humborg, C., Mörth, C.-M., Sundbom, M., Borg, H., Blenckner, T., Giesler, R., Ittekkot, V., 2009. CO₂ supersaturation along the aquatic conduit in Swedish watersheds as constrained by terrestrial respiration, aquatic respiration and weathering. *Global Change Biology* 16, 1966–1978.

- Jørgensen, B.B., Bang, M., Blackburn, T., 1990. Anaerobic mineralization in marine sediments from the Baltic Sea-North Sea transition. *Marine Ecology Progress Series* 59, 39–54.
- Kim, H.-C., Lee, K., 2009. Significant contribution of dissolved organic matter to seawater alkalinity. *Geophysical Research Letters* 36.
- Korth, F., Deutsch, B., Liskow, I., Voss, M., 2011. Uptake of dissolved organic nitrogen by size-fractionated plankton along a salinity gradient from the North Sea to the Baltic Sea. *Biogeochemistry*, doi:10.1007/s10533-011-9656-1.
- Kuliński, K., Pempkowiak, J., 2011. The carbon budget of the Baltic Sea. *Biogeosciences* 8, 3219–3230.
- Löffler, A., Schneider, B., Schmidt, M., Nausch, G., 2011. Estimation of denitrification in Baltic Sea deep water from gas tension measurements. *Marine Chemistry* 125, 91–100.
- Millero, F.J., 1995. Thermodynamics of the carbon dioxide system in the oceans. *Geochimica et Cosmochimica Acta* 59, 661–677.
- Millero, F.J., Graham, T.B., Huang, F., Bustos-Serrano, H., Pierrot, D., 2006. Dissociation constants of carbonic acid in seawater as a function of salinity and temperature. *Marine Chemistry* 100, 80–94.
- Mucci, A., 1983. The solubility of calcite and aragonite in seawater at various salinities, temperatures, and one atmosphere total pressure. *American Journal of Science* 283, 780–799.
- Mörth, C.M., Humborg, C., Eriksson, H., Danielsson, Å, Rodriguez Medina, M., Löfgren, S., Swaney, D.P., Rahm, L., 2007. Modeling riverine nutrient transport to the Baltic Sea: a large-scale approach. *AMBIO: A Journal of the Human Environment* 36, 124–133.
- Omstedt, A., Edman, M., Claremar, B., Frodin, P., Gustafsson, E., Humborg, C., Hägg, H., Mörth, C.-M., Rutgersson, A., Schurges, G., Smith, B., Wällstedt, T., Yurova, A., 2012. Future changes in the Baltic Sea acid-base (pH) and oxygen balances. *Tellus B* 64.
- Rebsdorf, A., Thyssen, N., Erlandsen, M., 1991. Regional and temporal variation in pH, alkalinity and carbon dioxide in Danish streams, related to soil type and land use. *Freshwater Biology* 25, 419–435.
- Riley, J.P., 1965. The occurrence of anomalously high fluoride concentrations in the North Atlantic. *Deep-Sea Research* 12, 219–220.
- Rutgersson, A., Smedman, A., 2010. Enhanced air–sea CO₂ transfer due to water-side convection. *Journal of Marine Systems* 80, 125–134.
- Savchuk, O.P., 2010. *Large-Scale Dynamics of Hypoxia in the Baltic Sea*. Springer Berlin Heidelberg, Berlin, Heidelberg.
- Savchuk, O.P., Gustafsson, B.G., Müller-Karulis, B., 2012. BALTSEM - a marine model for the decision support within the Baltic Sea Region (Technical Report No. 7), BNI Technical Report Series.
- Schneider, B., Nausch, G., Nagel, K., Wasmund, N., 2003. The surface water CO₂ budget for the Baltic Proper: a new way to determine nitrogen fixation. *Journal of Marine Systems* 42, 53–64.

- Schneider, B., Kaitala, S., Raateoja, M., Sadkowiak, B., 2009. A nitrogen fixation estimate for the Baltic Sea based on continuous pCO₂ measurements on a cargo ship and total nitrogen data. *Continental Shelf Research* 29, 1535–1540.
- Schneider, B., 2011. The CO₂ System of the Baltic Sea: Biogeochemical Control and Impact of Anthropogenic CO₂, in: Schernewski, G., Hofstede, J., Neumann, T. (Eds.), *Global Change and Baltic Coastal Zones*. Springer Netherlands, Dordrecht, pp. 33–49.
- Tyrell, T., Schneider, B., Charalampopoulou, A., Riebesell, U., 2008. Coccolithophores and calcite saturation state in the Baltic and Black Seas. *Biogeosciences (BG)* 5, 485–494.
- Ulfso, A., Hulth, S., Anderson, L.G., 2011. pH and biogeochemical processes in the Gotland Basin of the Baltic Sea. *Marine Chemistry* 127, 20–30.
- Uppström, L.R., 1974. The boron/chlorinity ratio of deep-sea water from the Pacific Ocean. *Deep-Sea Research* 21, 161–162.
- Van Mooy, B.A.S., Fredricks, H.F., Pedler, B.E., Dyhrman, S.T., Karl, D.M., Koblížek, M., Lomas, M.W., Mincer, T.J., Moore, L.R., Moutin, T., Rappé, M.S., Webb, E.A., 2009. Phytoplankton in the ocean use non-phosphorus lipids in response to phosphorus scarcity. *Nature* 458, 69–72.
- Wanninkhof, R., 1992. Relationship between wind speed and gas exchange. *J. Geophys. Res* 97, 7373–7382.
- Wanninkhof, R., Asher, W.E., Ho, D.T., Sweeney, C., McGillis, W.R., 2009. Advances in Quantifying Air-Sea Gas Exchange and Environmental Forcing. *Annual Review of Marine Science* 1, 213–244.
- Weiss, R.F., 1974. Carbon dioxide in water and seawater: the solubility of a non-ideal gas. *Marine Chemistry* 2, 203–215.
- Weiss, A., Kuss, J., Peters, G., Schneider, B., 2007. Evaluating transfer velocity-wind speed relationship using a long-term series of direct eddy correlation CO₂ flux measurements. *Journal of Marine Systems* 66, 130–139.
- Wolf-Gladrow, D.A., Zeebe, R.E., Klaas, C., Körtzinger, A., Dickson, A.G., 2007. Total alkalinity: The explicit conservative expression and its application to biogeochemical processes. *Marine Chemistry* 106, 287–300.
- Yao, W., Millero, F.J., 1995. The chemistry of the anoxic waters in the Framvaren Fjord, Norway. *Aquatic Geochemistry* 1, 53–88.

Appendix A

Calculating pH and pCO₂

A simplified expression for alkalinity, ignoring the small contributions from e.g. phosphate and ammonia reads as follows (cf. Equation 2.3):

$$A_T = [HCO_3^-] + 2[CO_3^{2-}] + [B(OH)_4^-] + [OH^-] + [HS^-] - [H^+] \quad (A1)$$

This simplified expression will be used to show how pH and pCO₂ are calculated in the model. pH is calculated on the total hydrogen ion concentration scale (pH^{tot}), and $[H^+]$ in the expressions above is thus defined as the sum of free hydrogen ions and hydrogen sulphate:

$$[H^+] = [H^+]_F + [HSO_4^-] \quad (A2)$$

In order to calculate pH and pCO₂ from alkalinity and DIC, the first step is to express all alkalinity species as functions of $[H^+]$ (e.g. Dickson et al., 2007):

$$[HCO_3^-] = C_T \frac{K_1[H^+]}{[H^+]^2 + K_1[H^+] + K_1K_2} \quad (A3)$$

$$[CO_3^{2-}] = C_T \frac{K_1K_2}{[H^+]^2 + K_1[H^+] + K_1K_2} \quad (A4)$$

$$[B(OH)_4^-] = \frac{K_B B_T}{K_B + [H^+]} \quad (A5)$$

$$[OH^-] = \frac{K_W}{[H^+]} \quad (A6)$$

$$[HS^-] = \frac{K_{H_2S} H_2 S_T}{K_{H_2S} + [H^+]} \quad (A7)$$

The simplified expression for alkalinity then reads as follows:

$$A_T = \frac{K_1([H^+] + 2K_2)C_T}{([H^+]^2 + K_1[H^+] + K_1K_2)} + \frac{K_B B_T}{(K_B + [H^+])} + \frac{K_W}{[H^+]} + \frac{K_{H_2S} H_2 S_T}{(K_{H_2S} + [H^+])} - [H^+] \quad (A8)$$

The dissociation constants K_1 , K_2 , K_B , K_W , and K_{H_2S} are known functions of temperature and salinity (the pressure effect is ignored in BALTSEM). Dissociation constants are however only valid in certain salinity ranges. Consequently, it is crucial to use constants defined at suitable salinities. Except for the dissociation constant of hydrogen sulphide, the constants used in BALTSEM (Table A1) follow the recommendations for Baltic Sea salinities by Ulfsbo et al. (2011).

Table A1. Dissociation constants used in BALTSEM.

Parameter	Notation	Reference
Dissociation constants of carbonic acid	K_1, K_2	Millero et al. (2006)
CO ₂ solubility constant	K_0	Weiss (1974)
Auto-dissociation constant of water	K_W	Millero (1995)
Fluoride equilibrium constant	K_F	Dickson and Riley (1979)
Borate equilibrium constant	K_B	Dickson (1990)
Dissociation constant of ammonia	K_{NH_3}	Yao and Millero (1995)
Dissociation constants of phosphoric acid	K_{1P}, K_{2P}, K_{3P}	Yao and Millero (1995)
Dissociation constant of silicic acid	K_{Si}	Yao and Millero (1995)
Dissociation constant of hydrogen sulphide	K_{H_2S}	Löffler et al. (2011)

Parameterizations for total concentrations of borate and fluoride in relation to salinity (S) follow Riley (1965) and Uppström (1974) respectively:

$$B_T = 0.000416 \frac{S}{35} \quad (A9)$$

$$F_T = 0.000007 \frac{S}{35} \quad (A10)$$

In this case, differences in ionic composition between Baltic Sea water and oceanic water are neglected (and errors arising from this simplification are most likely very small compared to other errors).

The total concentration of hydrogen sulphide is simply equal to the modelled "negative oxygen concentration" converted to $\mu\text{mol kg}^{-1}$ and multiplied by -0.5:

$$H_2S_T = [H_2S] + [HS^-] = -0.5[O_2] \quad (A11)$$

The next step is to solve Equation A8 for $[H^+]$. There is no analytical solution, and instead an iterative method must be used (e.g. Newton-Raphson). With $[H^+]$ known, pH can be calculated according to its definition:

$$pH = -\log_{10}([H^+]) \quad (A12)$$

Finally, $p\text{CO}_2$ is determined using $[H^+]$ and the temperature and salinity dependent solubility constant K_0 :

$$pCO_2 = \frac{[CO_2^*]}{K_0} = \frac{C_T[H^+]^2}{K_0([H^+]^2 + K_1[H^+] + K_1K_2)}$$

(A13)

Appendix B

Calculating calcite and aragonite saturation states

The calcium concentration (mol kg⁻¹) in the central Baltic Sea is calculated as

$$[Ca^{2+}] = (0.331S + 0.392)/1000$$

(A14)

and in the Bothnian Bay as (cf. Tyrrell et al., 2008):

$$[Ca^{2+}] = (0.375S + 0.368)/1000$$

(A15)

The carbonate concentration (mol kg⁻¹) is defined in Equation A4. Calcite and aragonite saturation states are now calculated as

$$\Omega = \frac{[Ca^{2+}][CO_3^{2-}]}{K_{sp}}$$

(A16)

where K_{sp} is the solubility product for either calcite or aragonite (Mucci, 1983).